Research Square

Preprints are preliminary reports that have not undergone peer review.
They should not be considered conclusive, used to inform clinical practice,
or referenced by the media as validated information.

Gly-tRF Enhances LCSCs-Like Cells Stemness and Promotes EMT of HCC Cells via Targeting NDFIP2 and Activating AKT Signaling Pathway.

Yongqiang Zhou
Lanzhou University
Jinjing Hu
Lanzhou University School Of Life Sciences
Lu Liu
Lanzhou University
Mengchao Yan
Lanzhou University
Qiyu Zhang
Lanzhou University
Xiaojing Song
Lanzhou University
Yan Lin
Lanzhou University
Dan Zhu
Lanzhou University
Yongjian Wei
Lanzhou University
Zongli Fu
Lanzhou University
Liming Hu
Lanzhou University School Of Life Sciences
Yue Chen
Lanzhou University
Xun Li (lix@lzu.edu.cn)
Lanzhou University https://orcid.org/0000-0001-6862-7692

Primary research

Keywords: Hepatocellular carcinoma, Liver cancer stem cells, tRNA-derived fragments, NDFIP2, EMT, AKT

Posted Date: April 12th, 2021

DOI: https://doi.org/10.21203/rs.3.rs-198357/v1

License: This work is licensed under a Creative Commons Attribution 4.0 International License. Read Full License

Abstract

Background: The existence of liver cancer stem cells (LCSCs) and the occurrence of epithelial-mesenchymal transition (EMT) are generally considered to be the primary causes for migration and metastasis of Hepatocellular carcinoma (HCC). Accumulating evidences demonstrate that tRFs and tiRNAs, are an emerging category of regulatory RNA molecules derived from transfer RNA (tRNA), are dysregulated in in various human cancer types and play crucial roles. However, their impact on tumorigenesis is still in the exploratory stage, their roles and mechanisms in HCC and LCSCs are still unknown.

Methods: Quantitative real-time PCR (qRT-PCR) was performed to detect the expression of glycine tRNA-derived fragments (Gly-tRF) in HCC cell lines and tumor tissues. Inhibitor and mimic were performed to weaken and enhance the function of Gly-tRF. Flow cytometry and sphere formation assay to detect the representative surface markers (CD133, CD13, EpCAM, CD44) proportion and stemness of LCSCs. Transwell assay and scratched wound assay were performed to detect HCC cells migration. Western blot was used to detect the expression of EMT-related proteins. Dual luciferase reporter assay and signaling pathway analysis were performed to explore the underlying mechanism of Gly-tRF functions.

Results: Gly-tRF is highly expressed in HCC cell lines and tumor tissues, compared to L02 hepatocytes and adjacent normal tissues. Flow cytometry and sphere formation assay found that Gly-tRF mimic promotes LCSCs subpopulation proportion and LCSCs-like cells stemness. Next, functional experiments confirmed that Gly-tRF mimic promotes HCC cells migration and EMT. Consistently, Loss of Gly-tRF inhibits HCC cells migration and EMT. Mechanistically, Gly-tRF inhibits the level of NDFIP2 mRNA by binding to the NDFIP2 3' UTR. Importantly, overexpression of NDFIP2 can weaken the effect of Gly-tRF in promoting LCSCs-like cells sphere formation and HCC cells migration, NDFIP2 is the direct target of Gly-tRF. Signaling pathway exploration found that Gly-tRF enhances the abundance of phosphorylated AKT.

Conclusions: Gly-tRF promotes EMT of HCC cells and enhances LCSCs-like cells stemness via targeting NDFIP2 and activating AKT signaling pathway. The tRNA-derived fragments provide a new perspective of oncology research, and can be the direction of future oncology research.

1. Background

Hepatocellular carcinoma (HCC) is one of the most common malignant tumors, causing a global health burden[1]. In the past few decades, reasonable methods of prevention, monitoring, early detection, diagnosis and treatment have been developed[2]. However, the poor survival of HCC patients after radical resection is due to high invasiveness and intrahepatic metastasis[3].

Epithelial–mesenchymal transition (EMT) has been considered as a driver of cancer pathogenesis[4]. The existence of Liver Cancer Stem Cells (LCSCs) is generally considered to be the primary cause of HCC metastasis, malignant growth and treatment failure[5]. Convincing evidences show that the existence of cancer stem cells is responsible for cancer cells undergoing epithelial-mesenchymal transition[6]. Some surface markers expressed by LCSCs are often used to characterize the stemness, subpopulation and self-renewal ability of LCSCs. Representative LCSCs surface markers are CD133, CD13, CD44 and epithelial cell adhesion molecule (EpCAM)[7]. Elucidate the underlying mechanism of HCC metastasis and recurrence from the regulation of LCSCs and EMT are particularly important.

A newly discovered type of non-coding RNAs (ncRNAs) derived from pre-transfer RNA (tRNA) or mature tRNA by precise site-specific cutting named tRFs (tRNA-derived small RNA fragments) and tiRNAs (tRNA halves)[8]. Abnormal expression of tRFs and tiRNAs have been observed in many human diseases, including tumors, neurodegenerative diseases, metabolic diseases and infectious diseases[9, 10]. tRFs and tiRNAs have been detected in a variety of body fluids and tissues[11], their expression is highly abundant[12], heavily modified and not easily degraded, making them more stable than other sncRNAs and increasingly becoming a popular field of oncology research.

Accumulating evidences show that tRFs and tiRNAs play crucial roles in human tumors including breast cancer[13–16], prostate cancer[17, 18], colorectal cancer[19, 20] by participating in multiple biological functions, including gene expression and silencing, translation regulation and epigenetic regulation[21]. But the impact of tRFs and tiRNAs on the biological process of HCC remains unclear, the roles of tRFs and tiRNAs in LCSCs also need further research. A research has shown that glycine tRNA-derived fragments (Gly-tRF) expression is up-regulated in ethanol-fed mice and promotes alcoholic fatty liver disease (AFLD)[22]. AFLD is one of the early forms of liver injury. Some patients with simple steatosis can develop more severe forms of liver injury, including steatohepatitis, cirrhosis, and eventually HCC[23]. It is reasonable to speculate that Gly-tRF is upregulated in HCC and affects the function of HCC cells.

Here, we studied the roles of Gly-tRF in regulating EMT and liver cancer stem cell-like properties. Our results indicate that increased expression of Gly-tRF triggers EMT and liver cancer stem cell-like properties. Moreover, NDFIP2 was found to be a direct target of Gly-tRF. Importantly, overexpression of NDFIP2 can weaken the effect of Gly-tRF in promoting EMT and LCSCs-like cells sphere formation. Mechanistically, Gly-tRF promotes EMT by binding to the NDFIP2 3' UTR and activating the AKT signaling pathway. This study provides new evidence for the regulatory mechanism of tRNA-derived fragments in HCC and LCSCs.

2. Materials And Methods

Specimen collection, tissue microarray and immunohistochemical staining

15 cases of histologically confirmed tumors and matched adjacent non-tumor tissues came from HCC patients who underwent radical hepatectomy at Lanzhou University First Hospital. The study was approved by the hospital ethics committee and according to the institutional review committee's procedures, all patients had signed an informed consent form before the study. Purchased a tissue microarray containing 90 tumor tissues and matched adjacent non-tumor tissues from Shanghai Outdo Biotech Co., LTD (Shanghai, China).

All patients obtained written informed consent and were followed up for 5–6 years with clear prognostic information.

Perform immunohistochemical staining as previously described[24]. For immunohistochemical images, two experienced pathologists independently performed immunohistochemical staining scores according to the staining intensity (0: absence; 1: weak staining; 2: moderate staining; 3: strong staining) and the proportion of positive cells (0: negative; 1: < 25%%; 2: 26–50%; 3: > 50%). The staining intensity score plus the staining proportion score to calculate the final immunohistochemistry score. We defined immunohistochemical score 0 to 4 as low expression, and 5 to 6 as high expression.

Cell culture

Human liver cancer cell lines HepG2, Huh7 and HCCLM3 were purchased from China Center for Type Culture Collection (CCTCC, Wuhan, China) and were identified for short tandem repeats (STR). L02 hepatocytes were giftted from Zhongshan Hospital of Fudan University (Shanghai, China). Embryonic kidney cell line HEK-293T was a gift from Shanghai Genechem Co., Ltd. (Shanghai, China). All cells are grown in Dulbecco's modified Eagle's medium (DMEM, pH = 7.2, Gibco Company, Grand Island, NY, USA) containing 10% (v/v) fetal bovine serum (FBS, Hyclone, Logan, UT, USA). All cells were cultured in a humidified incubator (Thermo Fisher Scientific, Waltham, MA, USA) at 37 °C and 5% CO_2. All cells were tested for mycoplasma contamination.

RNA isolation

Harvested total RNA from cells and tissues using RNAiso Plus (Takara Holdings Inc., Kyoto, Japan) and follow the recommended manufacturer protocol to isolate total RNA. NanoDrop 2000 (Thermo Fisher Scientific, Waltham, MA, USA) was used to measure the quality and quantity of isolated RNA.

3'and 5'adaptor ligation, complementary DNA (cDNA) first strand synthesis and real time PCR

Heavy modifications contain in tRNA, such as 3'-aminoacyl, 3'-cP, m1A, m1G, and m3C methylations will seriously interfere with the reverse transcription. Therefore, conventional PCR methods may not be able to reflect the true expression of tRNA-derived fragments[25]. This work used rtStar™ tRF&tiRNA Pretreatment Kit (Arraystar Inc., Rockville, MD, USA. Cat #AS-FS-005) to remove various modifications of Gly-tRF before 3'and 5'adaptor ligation and cDNA synthesis. Synthesize cDNA using APExBIO first-strand cDNA synsthesis supermix (APExBIO Inc., Houston, TX, USA. Cat #K1073). All steps such as 3'-terminal deacylation, 3'-cP removal and 5'-P addition, demethylation and reverse transcription are carried out in accordance with the manufacturer's instructions. All reactions were performed on the Mx3000P QPCR system (Agilent Technologies Inc., Santa Clara, CA, USA) using the TB Green Premix Ex Taq II (Takara Holdings Inc., Kyoto, Japan) for real-time PCR according to the manufacturer's instructions. The primers are shown in Table 1. U6 or GAPDH expression for normalized endogenous control. The relative expression levels of Gly-tRF were analyzed by $2^{-\Delta\Delta CT}$ method.

Genes	Sequences
Gly-tRF	GCAUUGGUGGUUCAGUGGUAGAAUUCUCGC
	Forward: CATTGGTGGTTCAGTGGTAGAAT
	Reverse: AGTGCAGGGTCCGAGGTATT
Gly-tRF NC-inhibitor	TTCTCCGAACGTGTCACGT
Gly-tRF inhibitor	GCGAGAATTCTACCACTGAACCACCAATGC
Gly-tRF NC-mimic	CON238
Gly-tRF mimic	GCCTTGTTAAGTGCTCGCTTCGGCAGCACATATACTATGTTTGAATGAGGCTTCAGTACTTTACAGAATCGTTGCCTGCACATCTTGGAAACACTTGCTG
NDFIP2	Forward: TCAAACCCAGCACCGCAGATTG
	Reverse: CGCAGATAGCACCATACCTTCCAG
ABHD17B	Forward: GCTGCTTGGCTTGCTCTTAGGAC
	Reverse: TTCAACCCAGAGAGGCTCCACAG
KCNK10	Forward: ATGAAGTGGAAGACGGTGGTTGC
	Reverse: AGTGGCTGCTGTTGTTGGAAGAG
RNF103	Forward: TCATGGGTAAGGGCAGACTGGATG
	Reverse: AAAGAAGCAATCGGGTGGAAGAGG
CXXC4	Forward: TCCTCCTCCGCCTCCTCCTC
	Reverse: TGGCAATTTGAAACGCACTGTCTG
OXTR	Forward: GGTGGTGGCAGTGTTTCAGGTG
	Reverse: CAGGCAGCGAGCACGATGAC
WDR44	Forward: CAGTGGAAGTCAAAGGAGGTGGTG
	Reverse: GCCATGCTTGCGGTTAGGAGAG
OSER1	Forward: AGCACCAGTCAGAACAGCAACAG
	Reverse: TTGGGTAGCGTCAGAGGAGTCTTC
GAPDH	Forward: CCCACTAACATCAAATGGGG
	Reverse: CCTTCCACAATGCCAAAGTT
U6	Forward: CGCTTCGGCAGCACATATAC
	Reverse: GAACGCTTCACGAATTTGCGT

Table 2
Target genes of Gly-tRF predicted by miRDB

Gene	Gene description	Predicted target score	3´UTR length	Seed position
ABHD17B	Abhydrolase domain containing 17B	96	129	82
NDFIP2	**Nedd4 family interacting protein 2**	**96**	**3564**	**32**
KCNK10	Potassium two pore domain channel Subfamily K member 10	95	5427	676
RNF103	Ring finger protein 103	95	1564	896
CXXC4	CXXC finger protein 4	95	4106	2120,2783
OXTR	Oxytocin receptor	95	2569	1560, 2131, 2537
WDR44	WD repeat domain 44	94	974	860
OSER1	Oxidative stress responsive serine rich 1	94	1113	29

Cell transfection

HCCLM3 and HuH7 cells were seeded in 6-well plates (Corning Life Sciences, USA) at a density of 4×10^5 per well, when the cell fusion rate reached 40–50%, Gly-tRF negative control, Gly-tRF inhibitor, Gly-tRF mimic lentivirus were used transfected cells according to the manufacturer's instructions (Shanghai Genechem Co., Ltd. Shanghai, China). The sequences of all lentivirus products are shown in Table 1. After 72 h of transfection, the cells were cultured in complete medium containing 2ug/μL puromycin for 72 h. Gly-tRF stably transfected cells were used for subsequent experiments.

Proportion analysis of representative markers of liver cancer stem cells

HCC cells are prepared as a single cell suspension for staining. All antibodies used for staining were purchased from Miltenyi Biotec (Bergisch Gladbac, Germany), including phycoerythrin (PE)-conjugated CD133 antibody (Cat #130-110-962), PE-Vio770-conjugated CD13 antibody (Cat #130-120-727), allophycocyanin (APC)-conjugated EpCAM antibody (Cat #130-111-000), APC-Vio770-conjugated CD44 antibody (Cat #130-113-339) and REA control antibody (Cat # 130-113-438, 130-113-440, 130-113-434, 130-113-445, respectively). Detected the percentage of CD133, CD13, EpCAM, CD44 in the HCC cells population according to the manufacturer's instructions. In brief, 1×10^6 cells were centrifuged and resuspended in 98ul buffer, added 2μL antibody and incubated for 10min in the dark at 4℃. Washed with 1ml buffer, centrifuged at 300g for 10min, and resuspend in 400ul buffer for detection. Data was acquired by BD LSRFortessa. All samples were carried out in triplicate.

Sphere formation assays

2000 cells/well were planted on an ultra-low adhesion 6-well plate (Corning, USA), after 8-day incubation, spheres were counted and photographed (random 15 fields/well) on a stereo microscope (Olympus, Tokyo, Japan). The diameter of the spheres was measured by Image Pro Plus 6.0 software (Media Cybernetics Inc., Rockville, MD, USA), those clones with a diameter greater than 20μm were considered positive for spheres formation.

Transwell assays

Cell migration experiments were performed in a 24-well transwell chamber (0.8um pore size, Corning Life Sciences, Costar, USA). Stably transfected cells starved for 6 h in serum-free medium, trypsinized the cells and adjusted the cell concentration to 2×10^5 cells / mL after counting. 600 μL of complete medium containing 30% (v/v) serum was added to the lower chamber, 200 μL of cell suspension was added to the upper chamber, and cultured for 48 h. The cells in the upper chamber were taken and fixed with 4% paraformaldehyde (Solarbio, Beijing, China). After 0.5% crystal violet (Solarbio, Beijing, China) staining, they were observed under a microscope and photographed. All experiments were repeated three times.

Scratched wound assays

Trypsinized the stable transfected cells and seeded on a 6-well plate. When the cells fusion rate reached 90%, a 200 μL sterile pipette tip was used to uniformly make vertical intersection scratches in the 6-well plate. Washed off the cells 3 times with 1X PBS, and selected multiple random fields to observe the cell migration at 0h, 24h, 48h. Quantify the area and width of the scratches with Image-Pro Plus 6.0.

Protein extraction and western blotting analysis

The cells were washed with PBS, lysed with radio-immunoprecipitation assay (RIPA) lysis buffer (Beyotime, Shanghai, China) containing 1% 10 μM Phenylmethanesulfonyl fluoride (PMSF) and 1% phosphatase inhibitor. Quantitative protein concentration using bicinchoninic acid kit (BCA, Vazyme Biotechnology Co., Ltd., Nanjing, China). After protein reduction and denaturation, the equal amount of protein lysis and Page Ruler prestained protein ladder were loaded into 10% SDS-PAGE gel, then transferred to polyvinylidene fluoride (PVDF) membranes (Millipore, Billerica, MA, USA). The membranes were blocked with 5 % bovine serum albumin (BSA) and incubated (overnight, 4°C) with primary antibodies. Western blot was performed using antibodies that anti-NDFIP2(1:1000, Bioss antibodies Inc., Beijing, China. Cat # bs-19059R), anti-pan AKT (1:1000, Abcam, Cambridge, UK, Cat # ab8805), anti-AKT1 phospho (1:1000, Abcam, Cat # ab66138), anti-N cadherin (1:1000, Abcam, Cat # ab18203), anti-E cadherin (1:10000, Abcam, Cat # ab40772). After washings with TBS-T, membranes were incubated with the secondary antibody for 1 hour at room temperature. Protein bands are visualized with Western chemiluminescent HRP substrate (Millipore, Billerica, MA, USA). Anti-β-actin antibody (1:2000, Sigma, USA) is used as an internal control to ensure the equal amount of protein loading.

Immunofluorescence staining

Stably transfected cells grow overnight on glass coverslips. The cells were fixed with 4% paraformaldehyde for 10 minutes at room temperature. Wash the cells 3 times with ice PBS. Incubate the cells with PBS (containing 0.3% Triton X-100) for 10 minutes. Wash the cells 3 times with PBS for 5 minutes each. Block cells with 3% BSA for 30 minutes at room temperature. Incubate cells with anti-NDFIP2 antibody (1:200, Bioss antibodies Inc., Beijing, China. Cat # bs-19059R) overnight at 4°C. Wash the cells 3 times with PBS-T, Then the cells were incubated with Cy5 conjugated Goat Anti-Rabbit IgG (1:400, Servicebio, Wuhan, China, GB27303) at room temperature in the dark for 60 minutes. 4', 6-Diamidino-2-phenylindole (DAPI, Servicebio) incubate the cells for 5 minutes. After washing with PBS, images were captured using a fluorescence microscope (Nikon Eclipse C1; Nikon Corporation). Fluorescence quantitative analysis using Image-Pro Plus 6.0.

Plasmid construction, transfection and luciferase assay

NDFIP2 overexpression plasmid (pcDNA3.1 + NDFIP2 OE), NDFIP2 3' UTR wild-type (NDFIP2 wt) and NDFIP2 3' UTR mutant-type (NDFIP2 mut) luciferase reporter plasmids were all constructed from TSINGKE (Beijing, China). Renilla luciferase reporter plasmid pRL-TK and pGL6 promoter empty vector (pGL6, Beyotime, Shanghai, China), NDFIP2 wt or NDFIP2 mut co-transfected into HEK-293T cells in each well using Exfect Transfection Reagent (Vazyme Biotechnology Co., Ltd., Nanjing, China) followed the manufacturer's instructions. In short, 50ng pRL-TK plasmid and 400ng NDFIP2 wt, NDFIP2 mut or pGL6 were added to Opti-MEM, then mixed with 1 μL liposome and incubated for 10 minutes at room temperature. 48 hours after transfection, the cells were lysed,

followed the dual-luciferase® report analysis system (Promega, Madison, WI, USA) to perform dual-reporter assays. GLOMAX 20/20 LUMINOMETER (Promega, Madison, WI, USA) was used to detect luciferase activity. All samples were carried out in triplicate. The same method was performed to transfect HCCLM3 cells using pcDNA3.1 + NDFIP2 OE and pcDNA3.1 empty plasmid (pcDNA3.1 + vector). In short, 3 μg pcDNA3.1 + NDFIP2 OE or pcDNA3.1 + vector and 9 μL liposomes were added to the cells. After 48 h of cultivation, follow-up experiments were performed.

Bioinformatics analysis

Download gene expression profiles and clinical data based on the TCGA XENA database(https://xena.ucsc.edu/) for screening differentially expressed genes (DEGs) between HCC tissues and matched non-tumor tissues. Performed Gene Ontology (GO) for DEGs.

Statistical analysis

GraphPad Prism 8 (La Jolla, CA, USA) was used for all statistical analyses and drafts. $P < 0.05$ was considered statistically significant. A Student's *t*-test or one-way ANOVA were used for groups comparisons of quantitative data.

3. Results

Gly-tRF expression is elevated in HCC

To evaluate the differential expression of Gly-tRF, 3 independent repeated experiments to measure the expression of Gly-tRF in L02 hepatocytes and HCC cells lines (HCCLM3, Huh7, HepG2) by quantitative real-time PCR (qRT-PCR). Our results showed that the expression of Gly-tRF in HCCLM3, Huh7, and HepG2 cells are higher than that in L02 cells (Fig. 1A). In 15 cases of HCC specimens, the expression of Gly-tRF in tumor tissues is elevated compared with adjacent non-tumor ones (Fig. 1B). Based on the online database OncotRF (http://bioinformatics.zju.edu.cn/)[26], the median expression level of Gly-tRF in tumor tissues of HCC patients is higher than that in normal tissues (755.06RPM vs 655.40RPM) (Fig. 1C). HCCLM3 and Huh7 cells were applied for subsequent experiments, based on their differences in cells invasiveness and the fold changes of Gly-tRF. To evaluate the effect of Gly-tRF on HCC cells functions, Gly-tRF negative control, Gly-tRF inhibitor,Gly-tRF mimic lentivirus were used transfected HCCLM3 and Huh7 cells. To confirm that Gly-tRF inhibitor does block the expression of Gly-tRF, after transfection of Gly-tRF inhibitor, qRT-PCR was used to detect the expression of Gly-tRF, which was reduced than that of transfected Gly-tRF NC-inhibitor in HCCLM3 and Huh7 cells (Fig. 1D, Fig. 1E). It also assessed whether Gly-tRF mimic transfection boosts Gly-tRF expression. After transfection of Gly-tRF mimic, enhanced expression of Gly-tRF was observed than that of transfected Gly-tRF NC-mimic in HCCLM3 and Huh7 cells (Fig. 1D, Fig. 1E).

Gly-tRF is involved in the maintenance of LCSCs-like properties

The high expression of LCSCs surface markers (CD133/CD13/EpCAM/CD44) are often considered to represent the properties of LCSCs. We sought to evaluate whether Gly-tRF affects the LCSCs-like properties. We first compared the proportion of CD133, CD13, EpCAM and CD44 in HCCLM3 and Huh7 cells transfected with Gly-tRF NC-mimic and Gly-tRF mimic using flow cytometry.

Interestingly, our results showed that compared with transfected Gly-tRF NC-mimic in HCCLM3 cells, the stably transfected Gly-tRF mimic has a higher percentage of CD13+, EpCAM + and CD44+ (Fig. 2A). But the percentage of CD133 + no statistical difference attributable to discrete detection data (Fig. 2A). Similarly, Gly-tRF elevated the percentage of CD133+, CD13+, EpCAM + and CD44 + in Huh7 cells (Fig. 2C). It suggests that Gly-tRF expression may be involved in the regulation of LCSCs.

Next, the effect of Gly-tRF on the self-renewal potential of LCSCs was further investigated by sphere formation assays. Consistently, cells transfected with Gly-tRF mimic have a higher LCSCs sphere formation efficiency than cells transfected with Gly-tRF NC-mimic (Fig. 2B, Fig. 2D). Our data indicate that in human HCC, Gly-tRF plays a role in the maintenance of LCSCs-like properties.

Gly-tRF intensifies migration and EMT of HCC cells

Based on the above experimental results that Gly-tRF promotes maintenance of LCSCs-like properties, a large amount of credible evidence shows the driving role of cancer stem cells in tumor migration and spread[27]. Next, we evaluated the effect of Gly-tRF on the migration of HCCLM3 and Huh7 cells.

Through transwell assay, we observed that the number of migrated cells increased after Gly-tRF mimic transfection, and the number of migrated cells decreased after Gly-tRF inhibitor transfection, compared to that of the Gly-tRF NC transfection (Fig. 3A-3B, Fig. 3E-3F) in HCCLM3 and Huh7 cells.

Scratched wound assay was used to confirm the effect of Gly-tRF on HCC cells migration. Our results showed that Gly-tRF mimic transfection speeds up the wound healing area, while Gly-tRF inhibitor transfection slows down the wound healing area at 48 hours, compared to Gly NC transfection (Fig. 3C-3D, Fig. 3G-3H) in HCCLM3 and Huh7 cells.

Tumor metastasis is often accompanied by the occurrence of EMT, next, we used western blot to detect the abundance of core markers in EMT. The results showed that the abundance of N-cadherin in the cells transfected with Gly-tRF inhibitor decreased, while the abundance of E-cadherin increased. Consistently, Gly-tRF mimic transfection correspondingly reversed this change (Fig. 3I-3J).

Taken together, these results demonstrate that Gly-tRF as a cancer-promoting factor, it plays critical roles in HCC by promoting migration and EMT.

Gly-tRF inhibits NDFIP2 3'UTR luciferase reporter activity

Studies have shown that tRNA-derived fragments inhibits target genes biological functions by binding to the 3' UTR of the target genes exert a function similar to miRNA[28, 29]. Online database miRDB allows to use user-provided tRNA-derived fragments sequences for custom target prediction[30], to investigate the regulation of Gly-tRF on downstream genes, we used miRDB to predict several Gly-tRF target genes(Table.2). Then, we evaluated the effect of Gly-tRF mimic transfection on the expression of selected predicted target genes by qRT-PCR. Nedd4 family interacting protein 2(NDFIP2) is an activator of Nedd4 family E3 ubiquitin ligase[31],its mRNA level decreases when Gly-tRF mimic transfection(Fig. 4A). Interestingly NDFIP2 gene was reduced in 371 HCC tissues, compared with 50 normal liver tissues by matching the expression level of NDFIP2 in the TCGA database (https://portal.gdc.cancer.gov/) and low expression implies a poor prognosis of HCC based on Kaplan-Meier Plotter database (http://kmplot.com/) (Fig. 4B-4C). Immunohistochemistry was used to verify the expression of NDFIP2 in HCC, the results showed that NDFIP2 protein expression in tumor tissues was lower in 58/84 (69%) samples, 17/84 (20%) had no difference, and only 9/84 (11%) were higher than that in non-tumor tissues adjacent to cancer (Fig. 4D). We initially identified NDFIP2 as a candidate target for Gly-tRF based on the above data and analysis. To determine whether Gly-tRF regulates the expression of selected target genes by binding to the seed sequence of NDFIP2 3' UTR, we used pGL6 as a vector to construct NDFIP2 3' UTR wild-type (NDFIP2 wt) and NDFIP2 3' UTR mutant (NDFIP2 mut) luciferase reporter plasmids (Fig. 4E). Our results show that luciferase activity is reduced when Gly-tRF mimic and NDFIP2 wt reporter plasmid were co-transfected HEK-293T cells (Fig. 4F). However, NDFIP2 wt reporter plasmid co-transfected with Gly-tRF NC-mimic, pGL6 empty vector and NDFIP2 mut reporter plasmid co-transfected with Gly-tRF NC-mimic, and pGL6 empty vector and NDFIP2 mut reporter plasmid co-transfected with Gly-tRF mimic are all did not inhibit the luciferase activity (Fig. 4F).

we detected the effect of Gly-tRF mimic transfection on the expression level of NDFIP2 protein by immunofluorescence and western blot. When transfected with Gly-tRF mimic, the expression level of NDFIP2 protein was inhibited (Fig. 5A-5C). Our experiments demonstrate that Gly-tRF inhibits the expression of NDFIP2 by specifically binding to NDFIP2 3' UTR.

Overexpression of NDFIP2 partially reverses the HCC-promoting effect of Gly-tRF

Next, we further investigated whether the overexpression of NDFIP2 terminate or reverse the promotion of Gly-tRF on the migration of HCC cells and liver cancer stem cell-like properties. We constructed the NDFIP2 overexpression plasmid, when the NDFIP2 overexpression plasmid was transfected in HCCLM3 cells, the expression of NDFIP2 mRNA and NDFIP2 protein were increased through qRT-PCR and western blot verification (Fig. S1B-S1C). Our results showed that

overexpression of NDFIP2 will responsibly reverse the LCSCs sphere formation efficiency caused by Gly-tRF in HCCLM3 cells (Fig. 6A-6B). Consistently, the NDFIP2 overexpression plasmid co-transfected with Gly-tRF mimic will terminate Gly-tRF induced cell migration and expression of EMT-related markers in HCCLM3 cells (Fig. 6C-6G). These data common indicated that Gly-tRF as a cancer-promoting factor by inhibiting NDFIP2.

Gly-tRF/NDFIP2 functions through activating the AKT signaling pathway

Next, our aimed to identify the signaling pathways where the Gly-tRF/NDFIP2 functions. Through GO molecular function (GO-MF) analysis, we found that the Gly-tRF/NDFIP2 is mainly involved in ubiquitin protein ligase activity and phosphatidylinositol 3 – kinase (PI3K) activity (Fig. 7A).

Previous studies have shown that the depletion of NDFIP2 can inhibit AKT activation, promote Hela cell proliferation[32]. To investigate whether the AKT signaling pathway is involved in the function of NDFIP2, western blot was used to detect the phosphorylation levels of AKT. We found that in in Gly-tRF mimic transfected HCCLM3 cells, increased abundance of phosphorylated AKT and can be reversed by overexpression of NDFIP2(Fig. 7B).

In summary, the above data indicate that Gly-tRF negatively regulates the expression of NDFIP2, thereby activating the AKT signaling pathway to as a cancer-promoter of HCC (Fig. 7C).

Discussion

Transfer RNA derived fragments (tRFs and tiRNAs) play a key role in the mechanism of tumorigenesis and development to be supported by accumulating research evidences. However, the effect of tRFs and tiRNAs on HCC is still unknown, and further research is needed. In this regard, current research has identified a glycine tRNA-derived fragments (Gly-tRF) and revealed its interesting and exciting roles in promoting the migration and promoting HCC stem cell-like phenotype in HCC. More meaningfully, we confirmed that NDFIP2 is the direct target gene of Gly-tRF. Gly-tRF binds to NDFIP2 3' UTR, thereby inhibiting the translation of NDFIP2 mRNA. We also found that Gly-tRF induced HCC-promoting effects can be reduced by NDFIP2 overexpression. Moreover, mechanism studies have found that the function of the Gly-tRF /NDFIP2 is regulated by the AKT signaling pathway. Taken together, these results common support the important role of Gly-tRF in the mechanism of HCC, which is of great significance for the development of new research fields in the diagnosis and treatment strategies of HCC.

Previous studies have shown the biological function and potential molecular mechanism of dysregulated functional tRFs and tiRNAs in HCC. By deep-sequencing analysis of small RNAs identified a tRFs named tRF_U3_1, which is more abundant in Huh7 cell line and liver cancer tissue and negatively regulate viral gene expression[33]. High-throughput sequencing results of small RNAs in liver tissues of advanced hepatitis B or C and HCC showed that tRFs and tiRNAs are the most abundant in chronically infected liver, and its abundance has changed in HCC[34]. These growing evidences reveal the potential relationship between tRFs and HCC. In this study, we report a tRNA derived fragments, Gly-tRF, which up-regulated expression in HCC cell lines and HCC tissues. Furthermore, our results confirm that elevated Gly-tRF promotes HCC cell migration. Although the tRNA-derived fragments subtypes and tumor types are different, our results are consistent with previous studies, which indicate that elevated levels of tRNA-derived fragments act as cancer-promoting factors[35–37]. Researches on tRNA-derived fragments as tumor suppressors have been widely reported[19, 38, 39]. However, the number of human tRFs identified so far even exceeds the number of human protein-coding genes,the mechanism of tRFs involved in biogenesis has not yet been elucidated, and there

may be multiple mechanisms responsible[40]. Additionally, the expression abundance of tRFs are affected by the cellular context, and the transcription characteristics of tRFs are also related to personal attributes[40]. These variations make unlocking the function of tRFs extremely complicated. At present, tRFs represents an emerging, elusive, challenging and promising field, its regulation of biological activities requires more in-depth evaluation and more convincing evidence.

Our research establishes a link between tRNA-derived fragments and cancer stem cells. Results of the present study indicate that Gly-tRF increases the expression of markers representing stem cell-like phenotype. There have been discussions about the role of tRNA-derived fragments in stemness. In mouse tumor stem cell models, 5' tRNA accumulation regulates undifferentiated stem cell status in tumor through differential translation of proteins that regulate cell migration, adhesion, and stress response[41]. PUS7-mediated pseudouridylation activates tRFs biogenesis to control protein synthesis and stem cell fate determination, this post-transcriptional regulatory network directly affects tumorigenesis[42]. Above findings and our results together suggest that it is meaningful to integrate tRNA-derived fragments into the research of cancer stem cells.

The potential mechanism of tRNA-derived fragments involved in controlling the biological processes of HCC cells is multi-step and complex. Importantly, we found that the tumor-promoting effect of Gly-tRF on HCC cells depends on the AKT signaling pathway. Overexpression of NDFIP2 can weaken the tumor-promoting effect of Gly-tRF on HCC cells and restore the abundance of phosphorylated AKT. Accumulating evidences also indicate the activation of the AKT signaling pathway in HCC biogenesis[43, 44]. NDFIP2 regulates the stability of its target proteins by activating E3 ubiquitin ligase [31], Our GO-MF and GSEA-KEGG analysis results also insinuate NDFIP2 is involved in ubiquitin mediated proteolysis. We speculate that NDFIP2 regulates the AKT signaling pathway through the ubiquitination of downstream target proteins. However, our current research has not verified this reasonable speculation, which will be our next focus.

Conclusions

Taken together, the results of this study reveal that Gly-tRF regulates migration of HCC cells and liver cancer stem cell-like properties through negative regulation of NDFIP2 and activating the AKT signaling pathway. In recent years, tRNA-derived fragments have become a research active spot as an emerging field, our research provides a new perspective on the underlying mechanism of tRNA-derived fragments in HCC, and emphasized the roles of tRNA-derived fragments in LCSCs. However, the underlying mechanisms of tRNA-derived fragments in disease biogenesis are complicated. More credible evidence is needed to verify this issue in the future.

Abbreviations

tRNA: transfer RNA; Gly-tRF: Glycine tRNA-derived fragments; HCC: Hepatocellular carcinoma; CSCs: Cancer stem cells; LCSCs: Liver cancer stem cells; NDFIP2: Nedd4 family interacting protein 2; EpCAM: Epithelial cell adhesion molecule; tRFs: tRNA-derived small RNA fragments; tiRNAs: tRNA halves; ncRNAs: non-coding RNAs; AFLD: Alcoholic fatty liver disease; CCTCC: China Center for Type Culture Collection; STR: Short tandem repeats; DMEM: Dulbecco's modified Eagle's medium; FBS: Fetal bovine serum; PBS: Phosphate belanced solution; qRT-PCR: Quantitative real-time polymerase chain reaction; DAPI: 4',6-diamidino-2-phenylindole; PE: Phycoerythrin; APC: Allophycocyanin; Opti-MEM: Optimized minimum essential medium; RIPA: Radio Immunoprecipitation Assay; PMSF: Phenylmethanesulfonyl fluoride; SDS: sodium dodecyl sulfate; PAGE: polyacrylamide gel electrophoresis; BSA: Bovine serum albumin; TBS-T: Tris buffered saline tween; HRP: Horseradish Peroxidase; 4', 6-Diamidino-2-phenylindole: DAPI; TCGA: The Cancer Genome Atlas; DEGs: Differentially expressed genes; GO: Gene Ontology; ANOVA: Analysis of Variance; NC: Negative control; 3'-UTR: 3'-untranslated regions; GO-MF: GO molecular function; PI3K: Phosphatidylinositol 3–kinase; AKT: Protein Kinase B; JNK: c-Jun N-terminal kinase; PUS7: Pseudouridine synthase 7.

Declarations

Acknowledgements

We would like to thank the other members of this laboratory for their help and support. Thanks to the School of Life Sciences, Lanzhou University for the convenience of using experimental equipment.

Authors' contributions

XL, YZ and JH: Experiment conception and implementation. YZ, JH and LL: Data analysis. YZ and LL: Draft manuscript. JH, MY, QZ, XS: Technical guidance, experimental suggestions and specimen collection. YL, YW, ZF and DZ: Academic contributions and manuscript revision. LH and YC: Flow cytometry implementation. XL: Fund support.

Funding

This work was supported by the National Natural Science Foundation of China (Grant Number 82060119), and Gansu Province Science and Technology Planning Project (Grant Number 18JR2TA018), and Major Science and Technology Project of Gansu Province (Grant Number 1602FKDA001), and Gansu Province Health Industry Scientific Research Project (Grant Number GSWSKY-2015-49).

Availability of data and materials

All data supporting this research are included in the article and supplementary materials

Ethics approval and consent to participate

The study was approved by the hospital ethics committee and according to the institutional review committee's procedures, all patients had signed an informed consent form before the study.

Consent for publication

All authors read and approved the final manuscript.

Competing interests

All authors declare no conflicts of competing interest in this paper.

References

1. Llovet JM, Kelley RK, Villanueva A, Singal AG, Pikarsky E, Roayaie S, Lencioni R, Koike K, Zucman-Rossi J, Finn RS. Hepatocellular carcinoma. Nat Rev Dis Primers. 2021;7(1):6.
2. Kulik L, El-Serag HB. Epidemiology and Management of Hepatocellular Carcinoma. Gastroenterology. 2019;156(2):477–91. e471.
3. Krishnan MS, Rajan Kd A, Park J, Arjunan V, Garcia Marques FJ, Bermudez A, Girvan OA, Hoang NS, Yin J, Nguyen MH, et al: **Genomic analysis of Vascular Invasion in Hepatocellular Carcinoma (HCC) Reveals Molecular Drivers and Predictive Biomarkers**. *Hepatology* 2020.
4. Yang J, Antin P, Berx G, Blanpain C, Brabletz T, Bronner M, Campbell K, Cano A, Casanova J, Christofori G, et al. Guidelines and definitions for research on epithelial-mesenchymal transition. Nat Rev Mol Cell Biol. 2020;21(6):341–52.
5. Chai S, Ng KY, Tong M, Lau EY, Lee TK, Chan KW, Yuan YF, Cheung TT, Cheung ST, Wang XQ, et al. Octamer 4/microRNA-1246 signaling axis drives Wnt/beta-catenin activation in liver cancer stem cells. Hepatology. 2016;64(6):2062–76.
6. Zhou Q, Jin P, Liu J, Li S, Liu W, Xi S. HER2 overexpression triggers the IL-8 to promote arsenic-induced EMT and stem cell-like phenotypes in human bladder epithelial cells. Ecotoxicol Environ Saf. 2021;208:111693.
7. Wu J, Zhu P, Lu T, Du Y, Wang Y, He L, Ye B, Liu B, Yang L, Wang J, et al. The long non-coding RNA LncHDAC2 drives the self-renewal of liver cancer stem cells via activation of Hedgehog signaling. J Hepatol. 2019;70(5):918–29.
8. Sun C, Fu Z, Wang S, Li J, Li Y, Zhang Y, Yang F, Chu J, Wu H, Huang X, et al. Roles of tRNA-derived fragments in human cancers. Cancer Lett. 2018;414:16–25.
9. Park J, Ahn SH, Shin MG, Kim HK, Chang S. **tRNA-Derived Small RNAs: Novel Epigenetic Regulators**. *Cancers (Basel)* 2020, 12(10).
10. Shen Y, Yu X, Zhu L, Li T, Yan Z, Guo J. Transfer RNA-derived fragments and tRNA halves: biogenesis, biological functions and their roles in diseases. J Mol Med (Berl). 2018;96(11):1167–76.
11. Godoy PM, Bhakta NR, Barczak AJ, Cakmak H, Fisher S, MacKenzie TC, Patel T, Price RW, Smith JF, Woodruff PG, et al. Large Differences in Small RNA Composition Between Human Biofluids. Cell Rep. 2018;25(5):1346–58.
12. Chiou NT, Kageyama R, Ansel KM. Selective Export into Extracellular Vesicles and Function of tRNA Fragments during T Cell Activation. Cell Rep. 2018;25(12):3356–70 e3354.
13. Goodarzi H, Liu X, Nguyen HC, Zhang S, Fish L, Tavazoie SF. Endogenous tRNA-Derived Fragments Suppress Breast Cancer Progression via YBX1 Displacement. Cell. 2015;161(4):790–802.
14. Cui Y, Huang Y, Wu X, Zheng M, Xia Y, Fu Z, Ge H, Wang S, Xie H. Hypoxia-induced tRNA-derived fragments, novel regulatory factor for doxorubicin resistance in triple-negative breast cancer. J Cell Physiol. 2019;234(6):8740–51.
15. Telonis AG, Rigoutsos I. Race Disparities in the Contribution of miRNA Isoforms and tRNA-Derived Fragments to Triple-Negative Breast Cancer. Cancer Res. 2018;78(5):1140–54.
16. Sun C, Yang F, Zhang Y, Chu J, Wang J, Wang Y, Zhang Y, Li J, Li Y, Fan R, et al. tRNA-Derived Fragments as Novel Predictive Biomarkers for Trastuzumab-Resistant Breast Cancer. Cell Physiol Biochem. 2018;49(2):419–31.
17. Martens-Uzunova E, Jalava S, Dits N, Leenders Gv. **Diagnostic and prognostic signatures from the small non-coding RNA transcriptome in prostate cancer**. *Oncogene* 2012, 31(8):978–991.
18. Olvedy M, Scaravilli M, Hoogstrate Y, Visakorpi T. A comprehensive repertoire of tRNA-derived fragments in prostate cancer. Oncotarget. 2016;7(17):24766–77.
19. Huang B, Yang H, Cheng X, Wang D, Fu S, Shen W, Zhang Q, Zhang L, Xue Z, Li Y, et al. tRF/miR-1280 Suppresses Stem Cell–like Cells and Metastasis in Colorectal Cancer. Can Res. 2017;77(12):3194–206.
20. Li S, Shi X, Chen M, Xu N, Sun D, Bai R, Chen H, Ding K, Sheng J, Xu Z. Angiogenin promotes colorectal cancer metastasis via tiRNA production. Int J Cancer. 2019;145(5):1395–407.
21. Yu M, Lu B, Zhang J, Ding J, Liu P, Lu Y. tRNA-derived RNA fragments in cancer: current status and future perspectives. J Hematol Oncol. 2020;13(1):121.

22. Zhong F, Hu Z, Jiang K, Lei B, Wu Z. Complement C3 activation regulates the production of tRNA-derived fragments Gly-tRFs and promotes alcohol-induced liver injury and steatosis. Cell Res. 2019;29(7):548–61.
23. Lakshman R, Shah R, Reyes-Gordillo K, Varatharajalu R. Synergy between NAFLD and AFLD and potential biomarkers. Clin Res Hepatol Gastroenterol. 2015;39(Suppl 1):29–34.
24. Da Z, Gao L, Su G, Yao J, Fu W, Zhang J, Zhang X, Pei Z, Yue P, Bai B, et al. Bioinformatics combined with quantitative proteomics analyses and identification of potential biomarkers in cholangiocarcinoma. Cancer Cell Int. 2020;20:130.
25. Green JA, Ansari MY, Ball HC, Haqqi TM. tRNA-derived fragments (tRFs) regulate post-transcriptional gene expression via AGO-dependent mechanism in IL-1beta stimulated chondrocytes. Osteoarthritis Cartilage. 2020;28(8):1102–10.
26. Yao D, Sun X, Zhou L, Amanullah M, Pan X, Liu Y, Liang M, Liu P, Lu Y. OncotRF: an online resource for exploration of tRNA-derived fragments in human cancers. RNA Biol. 2020;17(8):1081–91.
27. Steinbichler TB, Savic D, Dudas J, Kvitsaridze I, Skvortsov S, Riechelmann H. Skvortsova, II: **Cancer stem cells and their unique role in metastatic spread**. Semin Cancer Biol. 2020;60:148–56.
28. Zhang S, Li H, Zheng L, Li H, Feng C. Identification of functional tRNA-derived fragments in senescenceaccelerated mouse prone 8 brain. AGING. 2019;11(22):10485–98.
29. Shen L, Tan Z, Gan M, Li Q, Chen L, Niu L, Jiang D, Zhao Y, Wang J, Li X, et al: **tRNA-Derived Small Non-Coding RNAs as Novel Epigenetic Molecules Regulating Adipogenesis**. *Biomolecules* 2019, 9(7).
30. Chen Y, Wang X. miRDB: an online database for prediction of functional microRNA targets. Nucleic Acids Res. 2020;48(D1):D127–31.
31. O'Leary CE, Riling CR, Spruce LA, Ding H, Kumar S, Deng G, Liu Y, Seeholzer SH, Oliver PM. Ndfip-mediated degradation of Jak1 tunes cytokine signalling to limit expansion of CD4 + effector T cells. Nat Commun. 2016;7:11226.
32. Mund T, Pelham HR. Regulation of PTEN/Akt and MAP kinase signaling pathways by the ubiquitin ligase activators Ndfip1 and Ndfip2. Proc Natl Acad Sci U S A. 2010;107(25):11429–34.
33. Cho H, Lee W, Kim GW, Lee SH, Moon JS, Kim M, Kim HS, Oh JW. Regulation of La/SSB-dependent viral gene expression by pre-tRNA 3' trailer-derived tRNA fragments. Nucleic Acids Res. 2019;47(18):9888–901.
34. Selitsky SR, Baran-Gale J, Honda M, Yamane D, Masaki T, Fannin EE, Guerra B, Shirasaki T, Shimakami T, Kaneko S, et al. Small tRNA-derived RNAs are increased and more abundant than microRNAs in chronic hepatitis B and C. Sci Rep. 2015;5:7675.
35. Honda S, Loher P, Shigematsu M, Palazzo JP, Suzuki R, Imoto I, Rigoutsos I, Kirino Y. Sex hormone-dependent tRNA halves enhance cell proliferation in breast and prostate cancers. Proc Natl Acad Sci U S A. 2015;112(29):E3816–25.
36. Zhang F, Shi J, Wu Z, Gao P, Zhang W, Qu B, Wang X, Song Y, Wang Z. A 3'-tRNA-derived fragment enhances cell proliferation, migration and invasion in gastric cancer by targeting FBXO47. Arch Biochem Biophys. 2020;690:108467.
37. Farina NH, Scalia S, Adams CE, Hong D, Fritz AJ, Messier TL, Balatti V, Veneziano D, Lian JB, Croce CM, et al. Identification of tRNA-derived small RNA (tsRNA) responsive to the tumor suppressor, RUNX1, in breast cancer. J Cell Physiol. 2020;235(6):5318–27.
38. Wang J, Ma G, Li M, Han X, Xu J, Liang M, Mao X, Chen X, Xia T, Liu X, et al. Plasma tRNA Fragments Derived from 5' Ends as Novel Diagnostic Biomarkers for Early-Stage Breast Cancer. Mol Ther Nucleic Acids. 2020;21:954–64.
39. Falconi M, Giangrossi M, Zabaleta ME, Wang J, Gambini V, Tilio M, Bencardino D, Occhipinti S, Belletti B, Laudadio E, et al. A novel 3'-tRNA(Glu)-derived fragment acts as a tumor suppressor in breast cancer by targeting nucleolin. Faseb j. 2019;33(12):13228–40.
40. Magee R, Rigoutsos I. On the expanding roles of tRNA fragments in modulating cell behavior. Nucleic Acids Res. 2020;48(17):9433–48.
41. Blanco S, Bandiera R, Popis M, Hussain S, Lombard P, Aleksic J, Sajini A, Tanna H, Cortes-Garrido R, Gkatza N, et al. Stem cell function and stress response are controlled by protein synthesis. Nature. 2016;534(7607):335–40.
42. Guzzi N, Ciesla M, Ngoc PCT, Lang S, Arora S, Dimitriou M, Pimkova K, Sommarin MNE, Munita R, Lubas M, et al. Pseudouridylation of tRNA-Derived Fragments Steers Translational Control in Stem Cells. Cell. 2018;173(5):1204–16 e1226.
43. Dimri M, Humphries A, Laknaur A, Elattar S, Lee TJ, Sharma A, Kolhe R, Satyanarayana A. NAD(P)H Quinone Dehydrogenase 1 Ablation Inhibits Activation of the Phosphoinositide 3-Kinase/Akt Serine/Threonine Kinase and Mitogen-Activated Protein Kinase/Extracellular Signal-Regulated Kinase Pathways and Blocks Metabolic Adaptation in Hepatocellular Carcinoma. Hepatology. 2020;71(2):549–68.
44. Rebouissou S, Nault JC. Advances in molecular classification and precision oncology in hepatocellular carcinoma. J Hepatol. 2020;72(2):215–29.

Figures

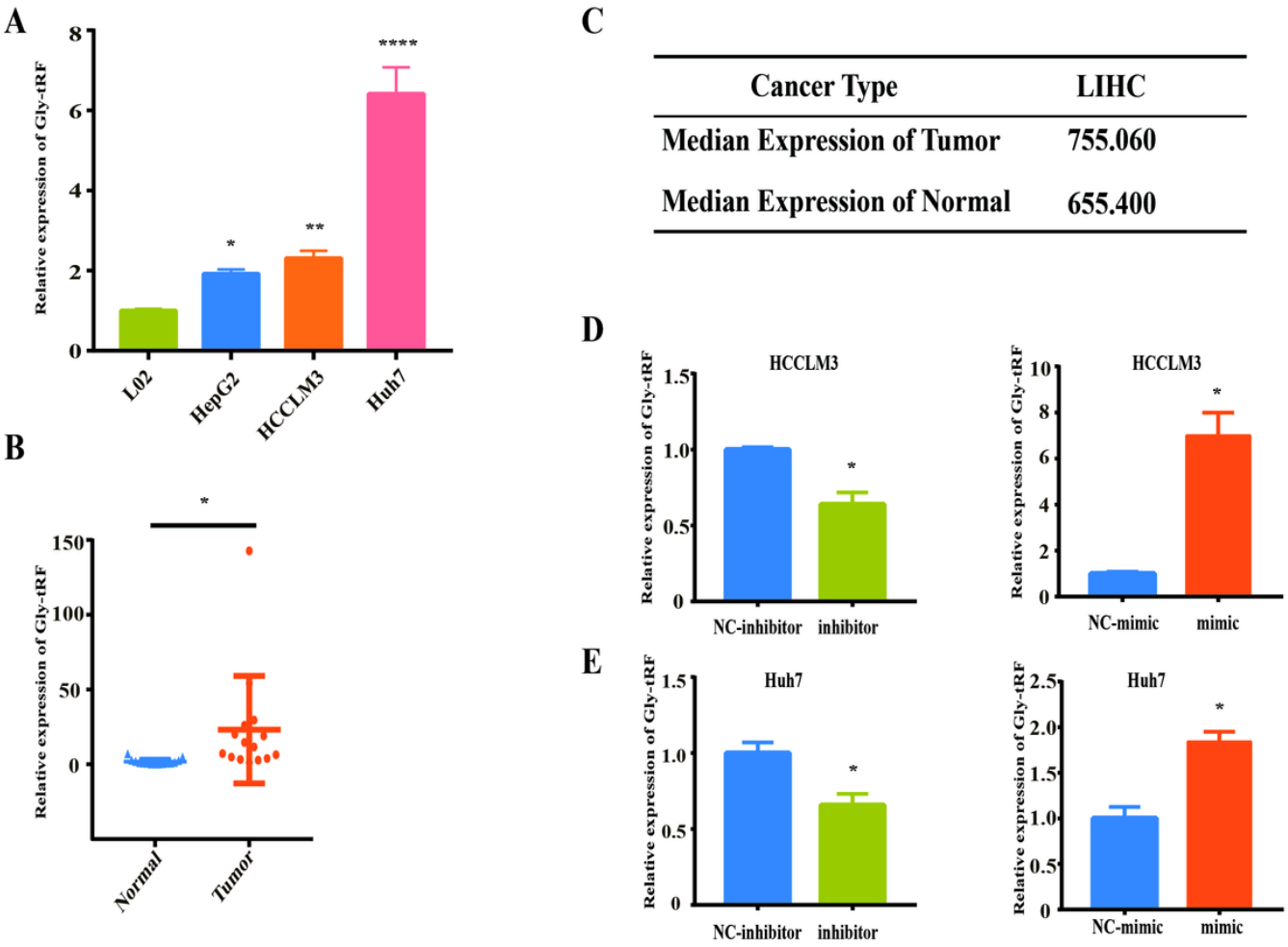

Figure 1

Gly-tRF expression is elevated in HCC A. Quantitative real-time PCR (qRT-PCR) shows that Gly-tRF is highly expressed in HCC cell lines (HCCLM3, Huh7, HepG2), compared to L02 hepatocytes. B. Scatter plots shows that in HCC specimens, the expression of Gly-tRF in tumor tissues is elevated compared with adjacent non-tumor ones (n = 15). C. Based on the online database OncotRF, the median expression level of Gly-tRF in tumor tissues of HCC patients is higher than that in normal tissues. LIHC: Liver hepatocellular carcinoma. D-E. Confirming of Gly-tRF enhancement or reduction transfected with Gly-tRF mimic or Gly-tRF inhibitor by qRT-PCR in HCCLM3 and Huh7 cells. Data are shown as mean ± SD. *P < 0.05, **P < 0.01, ****P < 0.0001.

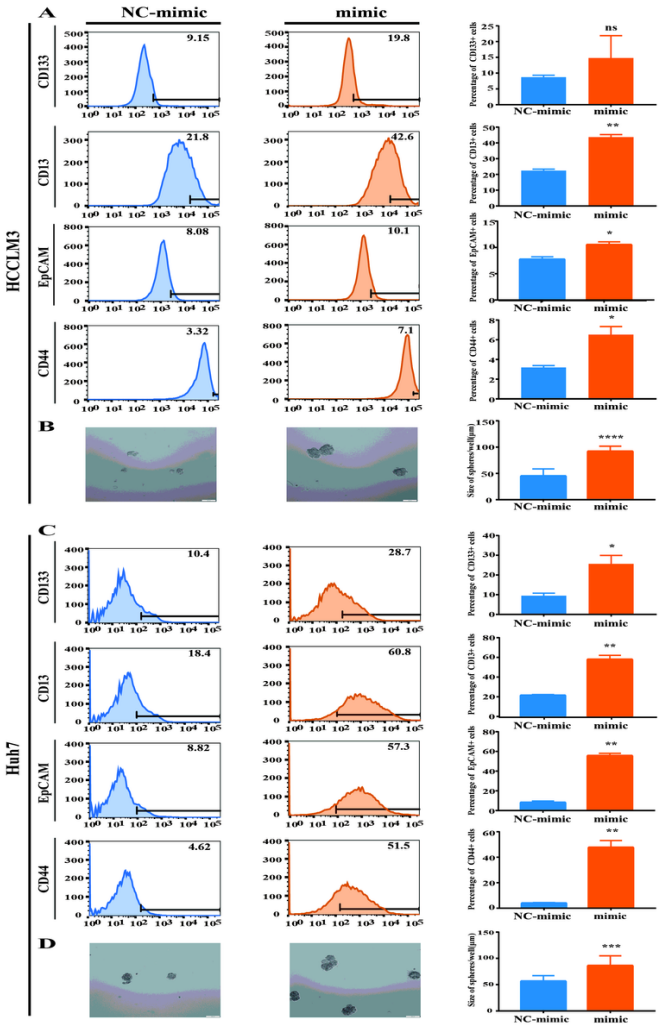

Figure 2

Gly-tRF is involved in the maintenance of LCSCs-like properties A, C. Flow cytometry to detect the percentage of representative liver cancer stem cell surface markers (CD133, CD13, EpCAM, CD44) in HCCLM3 and huh7 cells stably transfected with Gly-tRF NC-mimic and Gly-tRF mimic. The statistical graph shows result of three independent experiments. B, D. Sphere formation assay to reflect the sphere formation efficiency of those cells with liver cancer stem cell-like properties in HCCLM3 and huh7 transfected with Gly-tRF NC-mimic and Gly-tRF mimic. Scale bar = 100μm. The statistical graph shows the diameter of spheres in three independent experiments. Data are shown as mean ± SD. ns means no significance, *P < 0.05, **P < 0.01, ***P < 0.001, ****P < 0.0001.

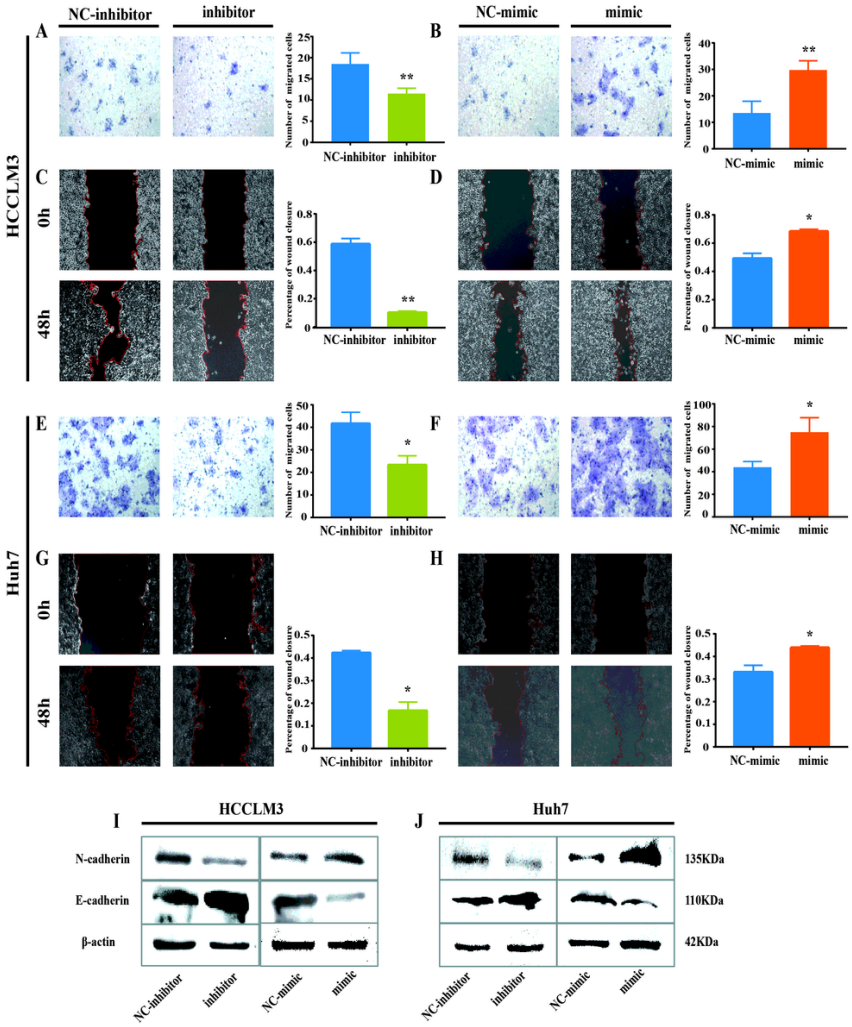

Figure 3

Gly-tRF intensifies migration and EMT of HCC cells A-B, E-F. Transwell assays is performed to evaluate cell migration in HCCLM3 and huh7 cells after Gly-tRF mimic or Gly-tRF inhibitor transfection. The statistical graph shows the average number of migrated cells in 5 random fields. Magnification, 200×. C-D, G-H. Scratched wound assays was used to confirm the effect of Gly-tRF on HCC cells migration. The percentage of wound closure represents the effect of Gly-tRF on the migration ability of cancer cells. Magnification, 100×. Data are shown as mean ± SD of three independent experiments. ns means no significance, *P < 0.05, **P < 0.01. I-J. Western blot was performed to detect the abundance of core markers(N-cadherin, E-cadherin) in EMT.

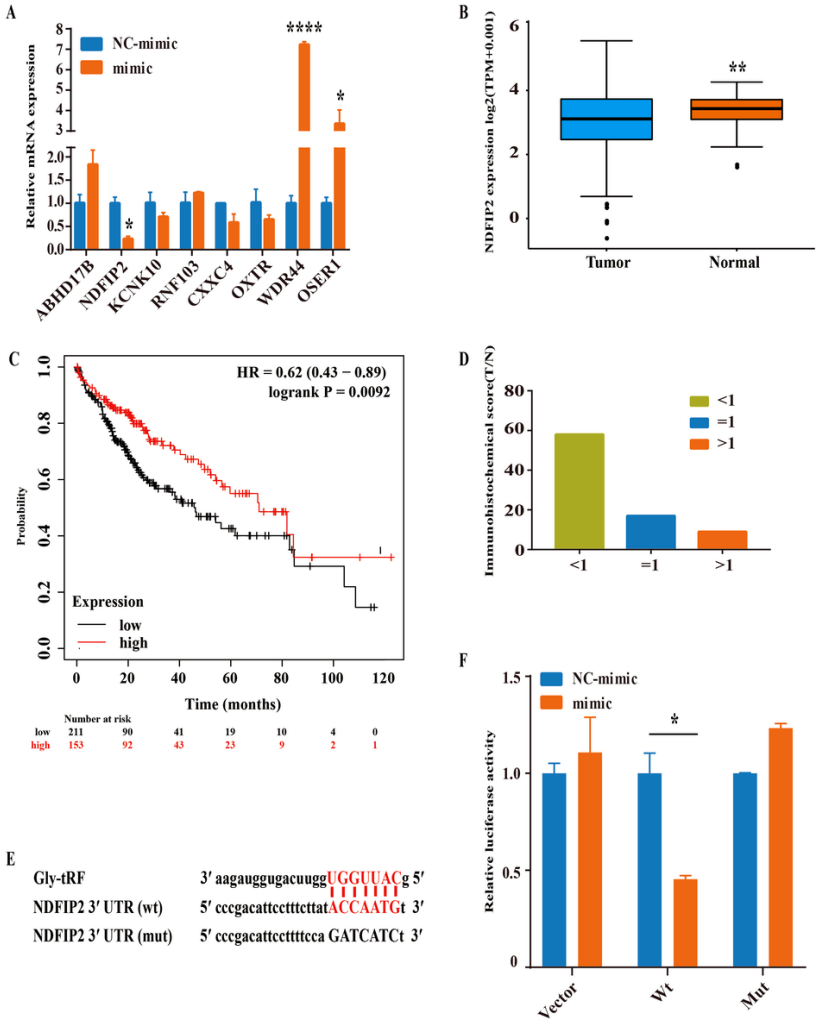

Figure 4

Gly-tRF inhibits NDFIP2 3'UTR luciferase reporter activity A. qRT-PCR was used to detect the mRNA expression of target genes predicted by miRDB in HCCLM3 cells transfected with Gly-tRF mimic. B. Expression of NDFIP2 gene in 371 HCC tissues and 50 normal liver tissues from the TCGA database. C. The expression of NDFIP2 is related to the prognosis of HCC Kaplan-Meier Plotter database. D. The expression of NDFIP2 in HCC was verified by immunohistochemistry. The relative expression of NDFIP2 protein is calculated by dividing the immunohistochemical score of the tumor tissue(T) by the immunohistochemical score of the matched non-tumor tissue(N) adjacent to the cancer. E. The sequence of Gly-tRF and the binding site of NDFIP2 3'UTR are shown. The sequence of the NDFIP2 mutant plasmid is also listed. F. Luciferase activity of cells transfected with pGL6 empty vector(vector), NDFIP2 3UTR wild-type(wt) and mutant plasmids(mut) co-transfected with Gly-tRF NC-mimic and Gly-tRF mimic in HEK-293T cells. Renilla luciferase activity (R value) was performed to correct and standardize firefly fluorescence activity (F value). Statistical graph data is expressed by F/R of three independent experiments. F. Western blot performed to detect the level of NDFIP2 protein in HCC cells stably transfected with Gly-tRF NC-mimic and Gly-tRF mimic. *P < 0.05, **P < 0.01, ****P < 0.0001.

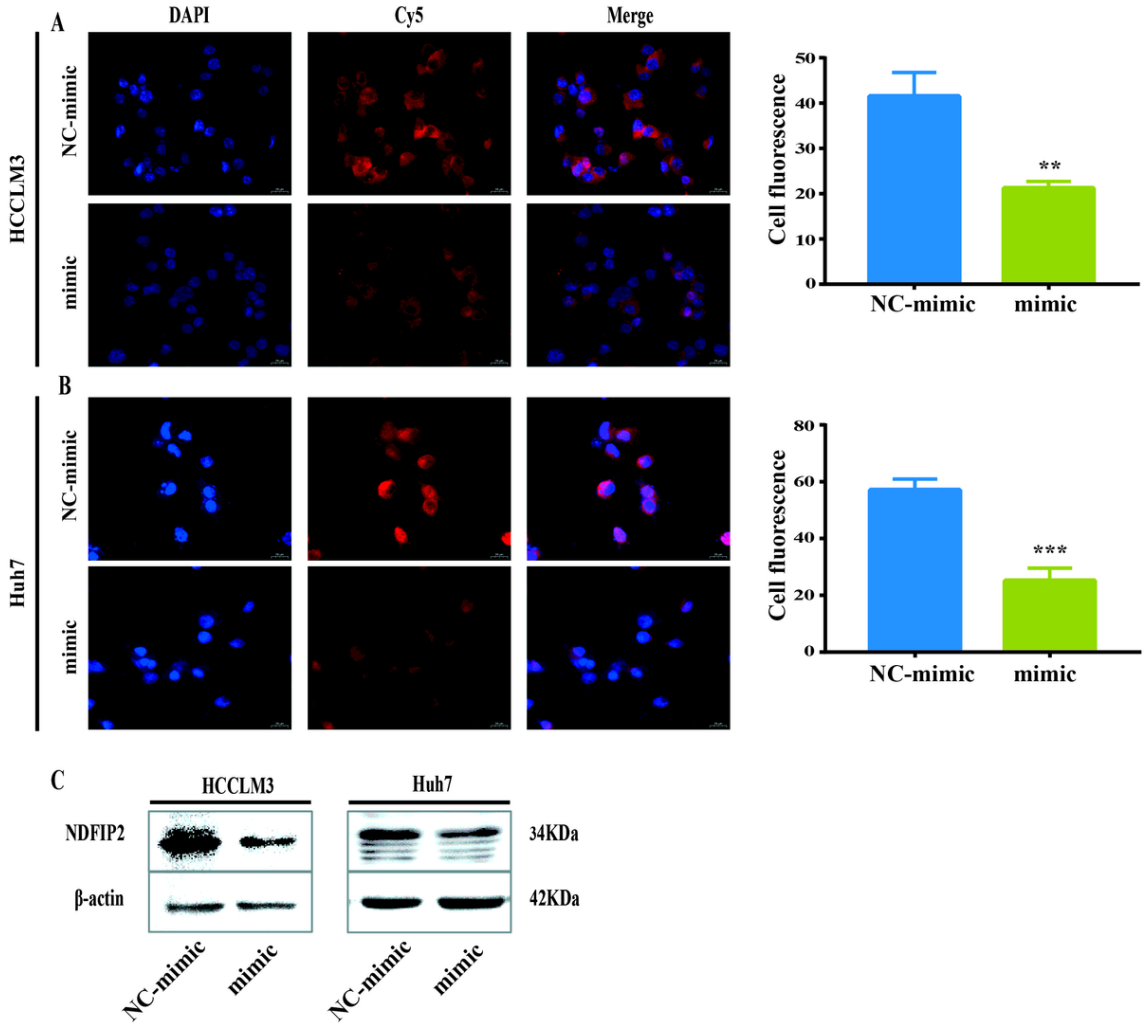

Figure 5

Gly-tRF inhibits the expression of NDFIP2 protein A-C. Immunofluorescence and western blot were performed to detect the level of NDFIP2 protein in HCC cells stably transfected with Gly-tRF NC-mimic and Gly-tRF mimic. The statistical graph shows the average value of cell fluorescence in 3 random fields. Magnification, 400×. Data are shown as mean ± SD. **P < 0.01, ***P < 0.001.

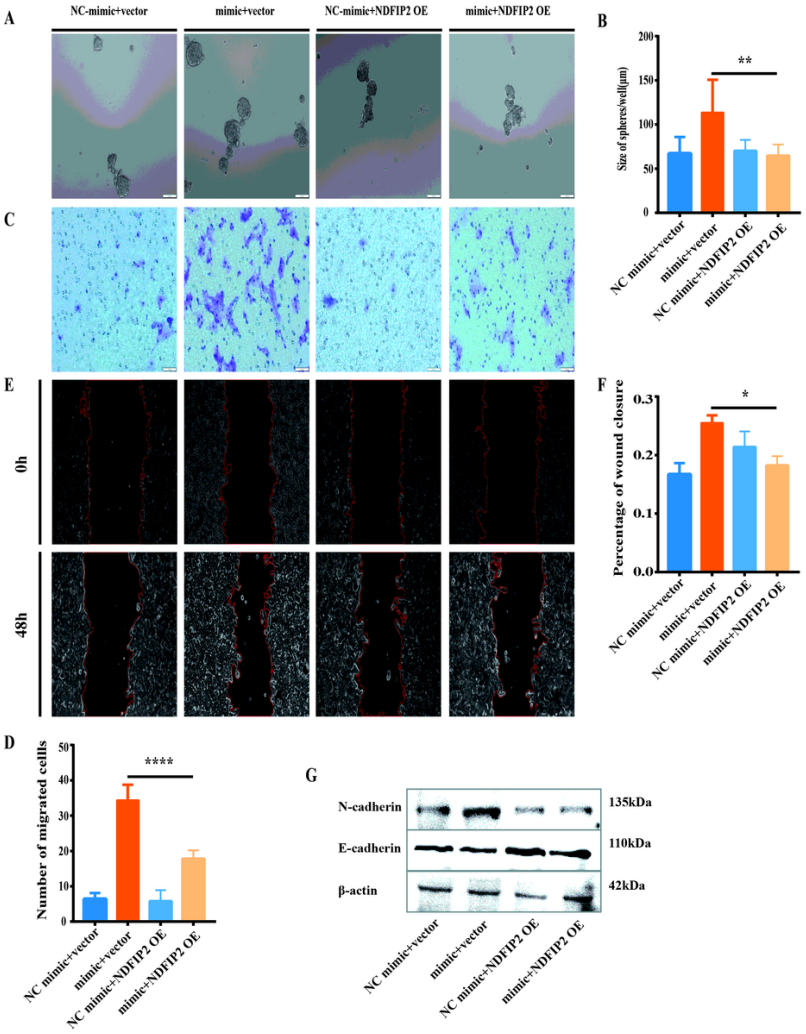

Figure 6

Overexpression of NDFIP2 partially reverses the HCC-promoting effect of Gly-tRF A-B. The sphere formation assay was performed to verify that the overexpression of NDFIP2 reversed CSCs sphere formation efficiency caused by Gly-tRF. Magnification, 100×. C-D. The transwell assay was performed to verify that the overexpression of NDFIP2 reversed the promotion of Gly-tRF on HCC cell migration. Magnification, 200×. E-F. Scratched wound assay was performed to verify that the overexpression of NDFIP2 reversed the promotion of Gly-tRF on HCC cell migration. Magnification, 100×. G. Western blot was performed to detect the abundance of core markers (N-cadherin, E-cadherin) in EMT. Data are shown as mean ± SD. *P < 0.05, **P < 0.01, ****P < 0.0001.

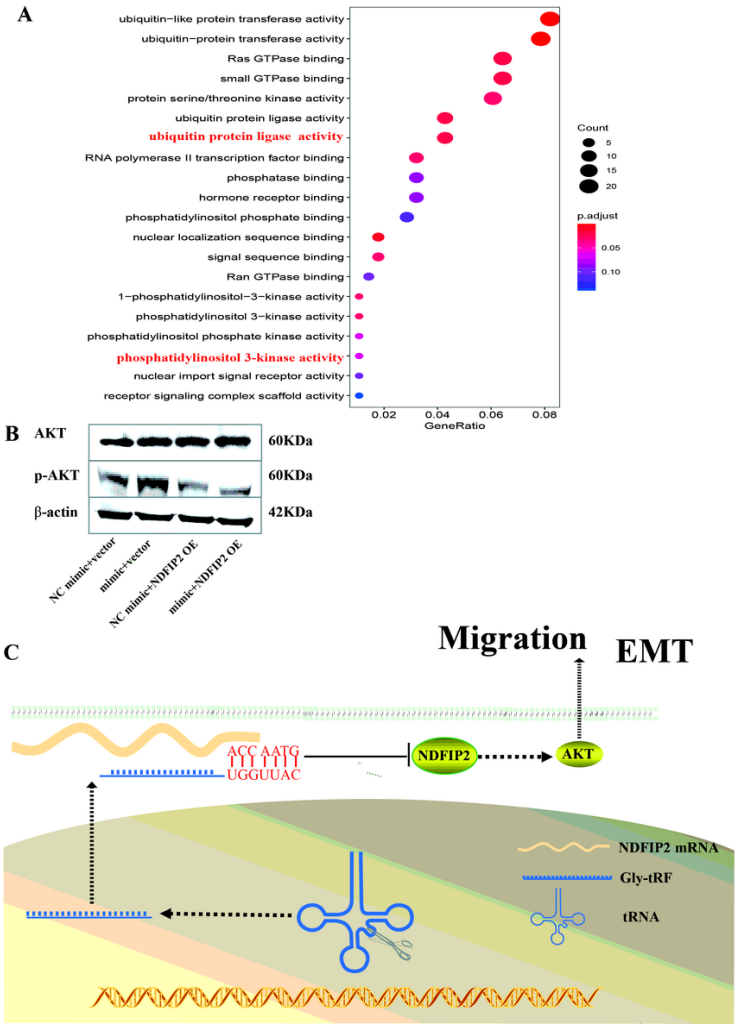

Figure 7

Gly-tRF/NDFIP2 functions through activating the AKT signaling pathway A. GO molecular function (GO-MF) analysis of NDFIP2 gene. B. Western blot was performed to detect the phosphorylation levels of AKT. C. Model diagram of Gly-tRF/NDFIP2 axis functioning in HCC.

Supplementary Files

This is a list of supplementary files associated with this preprint. Click to download.

- FigureS1A4.tif
- STRHCCLM3.pdf
- STRHepG2.pdf
- STRHuh7.pdf